Hindawi Publishing Corporation
Mathematical Problems in Engineering
Volume 2010, Article ID 686594, 30 pages
doi:10.1155/2010/686594

Research Article

Thermal Radiation Effects on Hydromagnetic Mixed Convection Flow along a Magnetized Vertical Porous Plate

Muhammad Ashraf,[1] S. Asghar,[1,2] and Md. Anwar Hossain[1]

[1] *Department of Mathematics, COMSATS Institute of Information Technology, Islamabad 54000, Pakistan*
[2] *Department of Mathematics, King Abdul Aziz University, Jeddah, Saudi Arabia*

Correspondence should be addressed to Muhammad Ashraf, ashrafm682003@yahoo.com

Received 15 October 2010; Accepted 20 December 2010

Academic Editor: Ekaterina Pavlovskaia

Aim of the present work is to investigate the effect of radiation on steady mixed convection boundary layer flow of viscous, incompressible, electrically conducting fluid past a semi-infinite magnetized vertical porous plate with uniform transpiration and variable transverse magnetic field along the surface. The equations governing the flow magnetic and temperature field are reduced to dimensionless convenient form using the free variable transformations and solved numerically by using finite difference method. Effects of physical parameters like Prandtl number, Pr, the conduction-radiation parameter R_d, magnetic field parameter S, magnetic Prandtl number Pm, mixed convection parameter λ, and the surface temperature, θ_w on the local skin friction coefficient Cf_x, local Nusselt number, Nu_x, and coefficient of magnetic intensity, Mg_x against the local transpiration parameter ξ are shown graphically. Later, the problem is analysed by using series solution for small and large values of ξ, and the results near and away from the leading edge are compared with numerical results obtained by finite difference method and found to be in good agreement.

1. Introduction

Thermal radiation effects on magnetohydrodynamics of an electrically conducting fluid flows are important in the context of space technology and processes involving high temperature. Physical interests of theses flows encountered in many engineering problems and industrial areas such as propulsion devices for missiles, aircraft, satellites, nuclear power plants, take place at high temperature and radiation effects play a significant role in designing them. One physical interest in this flow lies in the possibility of using such a field to shield a body from excessive heating and radiations. Here the literature survey is being started with the history of the work done by other authors along nonmagnetized, magnetized and then with porous surface and the radiation effects on these surface.

Greenspan and Carrier [1] was the first who investigated the flow of viscous, incompressible and electrically conducting fluid in the presence of a symmetrically oriented semi-infinite flat plate in which magnetic field assumed to be coincident with the ambient fluid velocity field. In this investigation fourier transformation together with asymptotic analysis had been incorporated and found that the velocity gradient at the plate approaches zero due to increase in the applied magnetic field intensity. Further contributions to the problem was added by Davies [2, 3] considering the fact that the flow is opposed by magnetodynamic pressure gradient along an nonmagnetized plate and concluded that for the magnetic field parameter (or Chandrashekhar number) $S \simeq 1$ the drag coefficient vanishes. Gribben [4] then considered an axisymmetric magnetohydrodynamic flow of an incompressible, viscous, electrically conducting fluid near a stagnation point considering that the magnetic field lines are circles and parallel to the surface. Later, Gribben [5] who investigated the magnetohydrodynamic boundary layer in steady incompressible flow under the influence of an external magnetic dynamic pressure gradient using the asymptotic analysis and found that the skin friction decreases with the increase of magnetic field. The boundary layer flow and heat transfer of hydromagnetic flow of viscous incompressible fluid flows past an electrically insulated semi-infinite flat plate in the presence of a uniform magnetic field parallel to the plate has been investigated by Ramamoorthy [6] numerically and found that the presence of the magnetic field increases both the momentum and thermal boundary layer thicknesses. On the other hand Tan and Wang [7] studied the effect of applied magnetic field on temperature distribution as well as on the recovery temperature due to the flow of a viscous incompressible electrically conducting fluid past a solid plane surface subject to uniform heat flux. They concluded that the values of recovery factor decreases with the increase of both magnetic field parameter S and magnetic Prandtl number Pm. Hildyard [8] found that the magnetic-field boundary condition used by Gribben was inappropriate and hence making the necessary correction obtained the appropriate asymptotic solutions for large and small values of the magnetic Prandtl number, Pm. Later, Chawla [9] studied the effect of free stream fluctuations on the flow over a semi-infinite plate, with an aligned magnetic field, using von Kármán-Pohlhausen technique and solution for low and high frequency ranges are developed. But, Ingham [10] studied the boundary layer flow on a semi-infinite flat plate placed at zero incidence to a uniform stream of electrically conducting gas with an aligned magnetic field at large distances from the plate. In this analysis the author observed that increasing magnetic field for a given Mach number, or decreasing the Mach number for a given magnetic field thickens the momentum and thermal boundary layer.

In all the above investigations, the surface along which the flow of the fluid were considered as nonmagnetized. In recent technological development it is necessary to distorted the attention towards magnetized surface, Glauert [11], first, studied the magnetohydrodynamic boundary layer in uniform flow past a magnetized plate for the small and large values of magnetic Prandtl number, Pm. The observation from this investigation, shows that the velocity and magnetic fields are valid for small value of magnetic field parameter S and for both smaller or larger value of magnetic Prandtl number Pm.

Chawla [12] studied the magnetohydrodynamics boundary layer in uniform flow past a semi-infinite magnetize plate, and a magnetic field fluctuating about a nonzero mean in the stream direction, is applied to the plate. He comments that in order to create a fluctuating magnetic field, one needs to join the plate in the manner of Glauert [11] with d.c and a.c generators placed in series. However, Chawla assuming the amplitude of the oscillating transverse magnetic field is much smaller than the uniform magnetic field at the surface. He also considered the basic steady flow using Karman-Pohlhausen technique, and obtained approximate solutions to both steady and oscillating part of the flow.

The effects of thermal radiation in different geometries have been discussed by several authors. In this respect, Ali et al. [13] focus on the effect of radiation interaction in boundary layer flow over horizontal surface. Arpaci [14], Cheng and Özişik [15], Sparrow and Cess [16] and highlight the thermal radiation effect with free convection from a heated vertical semi-infinite plate. Soundalgekar et al. [17] have studied radiation effects on free convection flow past a semi-infinite plate using the Colgey-Vincenti equilibrium model. Hossain and Takhar [18] have analyzed the effect of radiation using Rosseland diffusion approximation which leads to nonsimilar solutions for the forced and free convection flow of an optically dense viscous incompressible fluid past a heated vertical plate with uniform free stream velocity and surface temperature. The effect of conduction-radiation on oscillating natural convection boundary layer flow of optically dense viscous incompressible fluids along a vertical plate has been studied by Roy and Hossain [19]. Aboeldahab and Gendy [20] studied MHD free convection flow of gas past a semi-infinite vertical plate with variable thermophysical properties for high temperature difference by taking into consideration radiation effects and solved the problem numerically using the shooting method. Effects of thermal radiation on unsteady free convection flow past a vertical porous plate with Newtonian heating have recently been demonstrated by Mebine and Adigio [21], who obtained the analytical results by using the Laplace transform technique. Palani and Abbas [22] studied the combined effect of MHD and radiation on free convection flow past an impulsively started isothermal plate with Rosseland diffusion and solved the dimensionless governing equations numerically using the finite element method. Convective boundary layer flows are often controlled by injecting (blowing) or suction (withdrawing) fluid through porous bounding heating surface. This can lead to enhanced heating or cooling of system and can help to delay the transition from laminar to turbulent flow. Eichhorn [23], for example, obtained those power law variations in surface temperature and transpiration velocity which give rise to a similarity solution for the flow from a vertical surface. The case of uniform suction and blowing through an isothermal vertical wall was investigated first by Sparrow and Cess [24], they obtained a series solution which is valid near the leading edge. The problem was considered in more detail by Merkin [25], who obtained asymptotic solutions, valid at large distances from the leading edge, for both the suction and blowing. Using the method of matched asymptotic expansions, the next order correction to the boundary layer solution for this problem was obtained by Clarke [26], who obtained the range of applicability of the analysis by not invoking the the Boussinesq approximation. The effect of strong suction and blowing from general body shapes which admit a similarity solution has been given by Merkin [25]. A transformation of the equations for general blowing and wall temperature variations has been discussed by Vedhanayagam et al. [27]. The case of heated isothermal horizontal surface with transpiration has been discussed in some detail by Clarke and Riley [28] and then by Lin and Yu [29].

The above literature survey shows no existence of any study on the effects of thermal radiation on boundary layer flow of an electrically conducting fluid under both magnetic and buoyancy force along a magnetized porous plate. Hence in the present article the problem investigated is the thermal radiation effects on hydromagnetic mixed convection laminar boundary layer flow of a viscous, incompressible and electrically conducting fluid along a magnetized permeable surface with a variable magnetic field applied in stream direction at the surface. The boundary layer equations for the momentum, energy and magnetic field are reduced to convenient form for integration using appropriate transformations. The solutions of the transformed boundary layer equations are then simulated employing two methods, namely, (i) finite difference method and the (ii) asymptotic series solution for small and large value of local transpiration parameter $\xi = (V_0 x/\nu)/\mathrm{Re}_x^{1/2}$ that depends on the surface mass-flux, V_0, as well as the distance x measured from the leading edge of the plate. The pertinent physical parameters that dominate the flow and other physical quantities, such as the local skin-friction Cf_x, rate of heat transfer, Nu_x and the magnetic intensity Mg_x at the surface are the magnetic field parameter, S, and,conduction-radiation parameter R_d, Prandtl number Pr and the magnetic Prandtl number Pm and mixed convection parameter λ also with the surface temperature parameter θ_w.

2. Formulation of the Mathematical Model

We consider the radiation interaction on the laminar two-dimensional magnetohydrodynamic mixed convection flow of an electrically conducting, viscous and incompressible fluid past a uniformly heated vertical porous plate. The x-axis is taken along the surface and y-axis is normal to it. A schematic diagram illustrating the flow domain and the coordinate system is shown in Figure 1. In Figure 1 δ_M and δ_T stands for momentum and thermal boundary layer thicknesses. It is assumed that the surface temperature T_w of the plate is greater than the ambient fluid temperature T_∞

$$\frac{\partial u}{\partial x} + \frac{\partial v}{\partial y} = 0, \tag{2.1}$$

$$u\frac{\partial u}{\partial x} + v\frac{\partial v}{\partial y} = v\frac{\partial^2 u}{\partial y^2} + \frac{\overline{\mu}}{\rho}\left(H_x\frac{\partial H_x}{\partial x} + H_y\frac{\partial H_x}{\partial y}\right) + g\beta(T - T_\infty), \tag{2.2}$$

$$\frac{\partial H_x}{\partial x} + \frac{\partial H_y}{\partial y} = 0, \tag{2.3}$$

$$-\gamma\frac{\partial H_x}{\partial y} = \left(uH_y - vH_x\right), \tag{2.4}$$

$$u\frac{\partial T}{\partial x} + V\frac{\partial T}{\partial y} = \alpha\frac{\partial^2 T}{\partial y^2} - \frac{\partial q_r}{\partial y}, \tag{2.5}$$

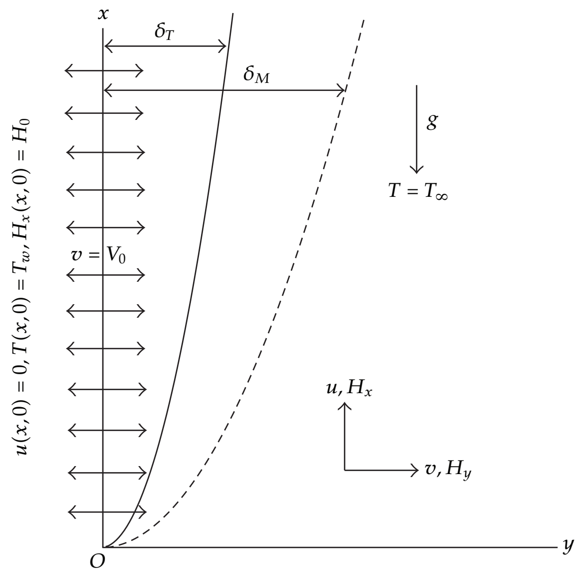

Figure 1: The coordinate system and flow configuration.

where

$$q_r = -K_r \frac{\partial T}{\partial y},$$
$$K_r = \frac{-16\sigma_s T^3}{3\alpha_R}, \tag{2.6}$$
$$\frac{\partial q_r}{\partial y} = -K_r \frac{\partial^2 T}{\partial y^2},$$

where u and v are fluid velocity components in x- and y-direction, respectively, H_x and H_y are the x- and y-components of magnetic field, q_r is the radiative heat flux in the y-direction, $\alpha, \overline{\mu}\ \rho, \nu$ and γ are the thermal diffusion, magnetic permeability, density, kinematic coefficient of viscosity and magnetic diffusivity of the medium. The solution of the above equations should satisfy the following boundary conditions:

$$u(x,0) = 0, \qquad \overline{v}(\overline{x},0) = \pm V_0, \qquad H_x(x,0) = H_w(x), \qquad T(x,0) = T_w,$$
$$u(x,\infty) = U_\infty(x), \qquad H_x(x,\infty) = 0, \qquad T(x,\infty) = T_\infty. \tag{2.7}$$

The nonlinearity of the momentum, hydromagnetic and energy equation makes it difficult to obtain a closed mathematical solution to the problem. However, by introducing the following nondimensional dependent and independent variables we have,

$$u = U_0\overline{u}, \qquad v = \frac{v}{L}\mathrm{Re}_L^{1/2}\overline{v}, \qquad \overline{x} = \frac{x}{L}, \qquad \overline{y} = \frac{y}{L}\mathrm{Re}_L^{1/2}y, \qquad H_x = H_0\overline{H}_x,$$
$$H_y = \frac{H_0}{\mathrm{Re}_L^{1/2}}\overline{H}_y, \qquad \theta = \frac{T - T_\infty}{\Delta T}, \tag{2.8}$$

where ΔT is the temperature difference. By using expression (2.8) in (2.1)–(2.15), we have

$$\frac{\partial \overline{u}}{\partial \overline{x}} + \frac{\partial \overline{v}}{\partial \overline{y}} = 0, \tag{2.9}$$

$$\overline{u}\frac{\partial \overline{u}}{\partial \overline{x}} + \overline{v}\frac{\partial \overline{v}}{\partial \overline{y}} = \frac{\partial^2 \overline{u}}{\partial \overline{y}^2} + S\left(\overline{H}_x\frac{\partial \overline{H}_x}{\partial \overline{x}} + \overline{H}_y\frac{\partial \overline{H}_x}{\partial \overline{y}}\right) + \lambda\overline{\theta}, \tag{2.10}$$

$$\frac{\partial \overline{H}_x}{\partial \overline{x}} + \frac{\partial \overline{H}_y}{\partial \overline{y}} = 0, \tag{2.11}$$

$$-\frac{1}{\mathrm{Pm}}\frac{\partial \overline{H}_x}{\partial \overline{y}} = \left(\overline{u}\overline{H}_y - \overline{v}\overline{H}_x\right), \tag{2.12}$$

$$\overline{u}\frac{\partial \overline{\theta}}{\partial \overline{x}} + \overline{V}\frac{\partial \overline{\theta}}{\partial \overline{y}} = \frac{1}{\mathrm{Pr}}\left[1 + \frac{4}{3R_d}(1 + (\theta_w - 1)\theta)^3\right]\frac{\partial^2 \overline{\theta}}{\partial \overline{y}^2}, \tag{2.13}$$

where

$$\mathrm{Re}_L = \frac{U_0 L}{\nu}, \qquad \mathrm{Gr}_L = \frac{g\beta\Delta T L^3}{\nu^2}, \qquad \mathrm{Pr} = \frac{\nu}{\alpha},$$
$$\lambda = \frac{\mathrm{Gr}_L}{\mathrm{Re}_L^2}, \qquad P_m = \frac{\upsilon}{\gamma}, \qquad \alpha = \frac{K}{\rho C_p}, \qquad S = \frac{\overline{\mu} H_0^2}{\rho U_0^2}, \qquad R_d = \frac{K\alpha_R}{4\sigma T_\infty^3}, \tag{2.14}$$

where Re_L is the Reynolds number, Gr_L the Grashof, number, R_d is the Plank number (radiation-conduction parameter), L the reference length, λ is the mixed convection parameter, Pr the Prandtl number and S the magnetic field parameter (also known as Chandrasekhar number), Pm is the magnetic Prandtl number, and α is the thermal diffusion. The corresponding boundary condition take the form:

$$\overline{u}(\overline{x},0) = 0, \qquad \overline{v}(\overline{x},0) = S_L, \qquad \overline{H}_x(\overline{x},0) = \overline{H}_w(x), \qquad \theta(x,0) = \overline{T}_w(\overline{x}),$$
$$\overline{u}(x,\infty) = 1, \qquad \overline{H}_x(x,\infty) = 0, \qquad \overline{T}(x,\infty) = 0. \tag{2.15}$$

In the above conditions $S_L = (V_0 L/\nu)\mathrm{Re}_L^{-1/2}$ is the transpiration parameter.

3. Method of Solutions

To get the set of equations in convenient form for integration, we will introduce the following one parameter group of transformation for the dependent and independent variables:

$$\overline{u} = U(\xi, Y), \quad \overline{v} = x^{1/2}(V + \xi), \quad \varphi = x^{1/2}\phi, \quad \overline{\theta} = x^{-1}\theta(\xi, Y),$$
$$Y = x^{-1/2}\overline{y}, \quad \xi = S_L\overline{x}^{1/2}, \quad \overline{H}_x = \frac{\partial\varphi}{\partial y}, \quad \overline{H}_y = -\frac{\partial\varphi}{\partial x}. \tag{3.1}$$

The ξ is the local distribution of the surface mass-flux. Here for suction (or withdrawal) ξ is positive and for injection (or blowing) of fluid ξ is negative and for solid surface ξ is zero. We further assume that the surface temperature $\overline{T}_w(\overline{x}) = \overline{x}^{-1}$ and the normal component of the magnetic field at the surface $\overline{H}_w(\overline{x}) = \overline{x}^{-1/2}$. where φ is the potential function that satisfies (2.11). By using this group of transformations, which satisfies equation of continuity and by using in (2.9)–(2.13): we have set of equations:

$$\frac{1}{2}\xi\frac{\partial U}{\partial \xi} - \frac{1}{2}Y\frac{\partial U}{\partial Y} + \frac{\partial V}{\partial Y} = 0, \tag{3.2}$$

$$\frac{1}{2}\xi U\frac{\partial U}{\partial \xi} + \left(V + \xi - \frac{1}{2}YU\right)\frac{\partial U}{\partial Y} - \frac{\partial^2 U}{\partial Y^2} - S\left[-\frac{1}{2}\phi\frac{\partial^2\phi}{\partial Y^2} + \frac{1}{2}\xi\left(\frac{\partial\phi}{\partial Y}\frac{\partial^2\phi}{\partial\xi\partial Y} - \frac{\partial^2\phi}{\partial Y^2}\frac{\partial\phi}{\partial\xi}\right)\right] - \lambda\theta = 0, \tag{3.3}$$

$$\frac{1}{\mathrm{Pm}}\frac{\partial^2\phi}{\partial Y^2} = \frac{1}{2}U\phi + \frac{1}{2}\xi U\frac{\partial\phi}{\partial\xi} + \left(V + \xi - \frac{1}{2}YU\right)\frac{\partial\phi}{\partial Y}, \tag{3.4}$$

$$\frac{1}{\mathrm{Pr}}\left[1 + \frac{4}{3R_d}(1 + (\theta_w - 1)\theta)^3\right]\frac{\partial^2\theta}{\partial Y^2} = \frac{1}{2}\xi U\frac{\partial\theta}{\partial\xi} + \left(V + \xi - \frac{1}{2}YU\right) - \frac{\partial\theta}{\partial Y} - U\theta. \tag{3.5}$$

The appropriate boundary conditions satisfied by the above system of equations are

$$U(\xi, 0) = V(\xi, 0) = 0, \quad \phi'(\xi, 0) = 1, \quad \theta(\xi, 0) = 1,$$
$$V(\xi, \infty) = 1, \quad \phi'(\xi, \infty) = 0, \quad \theta(\xi, \infty) = 0. \tag{3.6}$$

Once we know the solutions of the above equations, we readily can obtain the values of skin-friction, heat transfer and the normal magnetic intensity at the surface from the following relations in terms of skin-friction, Nusselt number and magnetic intensity from the following relations:

$$\mathrm{Re}_x^{1/2}\mathrm{Cf}_x = f''(\xi, 0),$$
$$\mathrm{Re}_x^{-1/2}\mathrm{Nu}_x = -\left(1 + \frac{4}{3R_d}\right)\theta'(\xi, 0), \tag{3.7}$$
$$\mathrm{Re}_x^{1/2}\mathrm{Mg}_x = -g(\xi, 0).$$

Now we will discretize the expressions (3.1)–(3.4) with boundary conditions given in (3.5), we have a new system of discretised form of equations as follows:

$$A_1 U_{i+1,j} + B_1 U_{i,j} + C_1 U_{i-1,j} = D_1, \tag{3.8}$$

where

$$\begin{aligned} A_1 &= 1 + \frac{1}{2}\left(V_{i,j} - \xi_i - Y_j U_{i,j}\right)\Delta Y, \\ B_1 &= -2 + \frac{1}{2}\frac{\xi_i}{\Delta\xi} U_{i,j}\Delta Y^2, \\ C_1 &= 1 - \frac{1}{2}\left(V_{i,j} - \xi_i - Y_j U_{i,j}\right)\Delta Y, \\ D_1 &= \left[\frac{S}{2\Delta\xi}(H_1)_{i,j}\left((H_1)_{i,j} - (H_1)_{i,j-1}\right) - \frac{1}{2}\frac{\xi_i}{\Delta\xi}U_{i,j}U_{i,j-1}\right]\Delta Y^2 \\ &\quad - \left[\frac{S}{4}\left((H_1)_{i+1,j} - (H_1)_{i-1,j}\right) + \frac{S}{2}\left((H_1)_{i,j} - (H_1)_{i-1,j}\right)(H_2)_{i,j}\right]\Delta Y, \end{aligned} \tag{3.9}$$

where $(H_1)_{i,j} = (\partial\phi/\partial y)_{i,j}$ and $(H_2)_{i,j} = (\partial\phi/\partial\xi)_{i,j}$.

Similarly for hydromagnetics equation we have

$$\begin{aligned} A_2\phi_{i+1,j} + B_2\phi_{i,j} + C_2\phi_{i-1,j} &= D_2, \\ A_2 &= \frac{1}{\text{Pm}} + \frac{1}{2}\left(V_{i,j} - \xi_i - Y_j U_{i,j}\right)\Delta Y, \\ B_2 &= -\frac{2}{\text{Pm}} - \frac{1}{2}\left(1 + \frac{\xi_i}{\Delta\xi}\right)U_{i,j}\Delta Y^2, \\ C_2 &= \frac{1}{\text{Pm}} - \frac{1}{2}\left(V_{i,j} - \xi_i - \frac{1}{2}Y_j U_{i,j}\right)\Delta Y, \\ D_2 &= -\frac{1}{2}\frac{\xi_i}{\Delta\xi}U_{i,j}\phi_{i,j-1}\Delta Y^2, \end{aligned} \tag{3.10}$$

and the discretised form of energy equation is of the form

$$A_3\theta_{i+1,j} + B_3\theta_{i,j} + C_3\theta_{i-1,j} = D_3, \tag{3.11}$$

where

$$A_3 = \frac{1}{\Pr}\left[1 + \frac{4}{3R_d}\left(1 + (\theta_w - 1)\theta_{i,j}\right)^3\right] + \frac{1}{2}\left(V_{i,j} - \xi_i - \frac{1}{2}Y_j U_{i,j}\right)\Delta Y,$$
$$B_3 = -\frac{2}{\Pr}\left[1 + \frac{4}{3R_d}\left(1 + (\theta_w - 1)\theta_{i,j}\right)^3\right] - \left(1 - \frac{1}{2}\frac{\xi_i}{\Delta\xi}\right)U_{i,j}\Delta Y^2,$$
$$C_3 = \frac{1}{\Pr}\left[1 + \frac{4}{3R_d}\left(1 + (\theta_w - 1)\theta_{i,j}\right)^3\right] - \frac{1}{2}\left(V_{i,j} - \xi_i - \frac{1}{2}Y_j U_{i,j}\right)\Delta Y, \qquad (3.12)$$
$$D_3 = -\frac{1}{2}\frac{\xi_i}{\Delta\xi}U_{i,j}\theta_{i,j-1}\Delta Y^2,$$

velocity can be calculated directly using equation of continuity (3.2) as shown below:

$$V_{i,j} = V_{i-1,j} - \frac{1}{2}\left(\xi\frac{\Delta y}{\Delta\xi} - Y_j\right)U_{i,j} + \frac{1}{2}\xi\frac{\Delta Y}{\Delta\xi}U_{i,j-1} - \frac{1}{2}Y_j U_{i-1,j}, \qquad (3.13)$$

where i and j denote the grid points along the X and Y directions, respectively. In order to find the numerical solution we have discretised the expressions (3.2)–(3.5) with boundary conditions (3.6) by using finite difference method, using backward difference for x-direction and central difference for y-direction out of which we get a system of tri-diagonal algebraic equations. These tri-diagonal equations are then solved by Gaussian elimination technique. The computation is started at $\xi = 0.0$, and then marches downstream implicitly. Once we know the solution of these equations, physical quantities of interest such as the coefficient of skin-friction, the coefficient of magnetic intensity, and the coefficient of rate of heat transfer at the surface may be calculated from

$$\mathrm{Re}_x^{1/2}\mathrm{Cf}_x = f''(\xi, 0), \qquad \mathrm{Mg}_x\mathrm{Re}_x^{1/2} = -\phi(\xi, 0), \qquad \frac{\mathrm{Nu}_x}{\mathrm{Re}_x^{1/2}} = -\left(1 + \frac{4}{3R_d}\right)\theta'(\xi, 0). \qquad (3.14)$$

4. Results and Discussions

In present investigation we have obtained the solutions of the nonsimilar boundary layer (3.2)–(3.5) with boundary conditions (3.6) that governs the flow of a viscous incompressible and electrically conducting fluid past a magnetized vertical porous plate with surface temperature by using the method discussed in the preceding section for a wide range of physical parameters, S, conduction-radiation parameter R_d, surface temperature θ_w, Prandtl number Pr, and mixed convection parameter λ, magnetic Prandtl number Pm, against ξ. Below we discuss the effects of the aforementioned physical parameters of the flow fields as well as on the local skin-friction coefficient $\mathrm{Re}_x^{1/2}\mathrm{Cf}_x$, the coefficient of surface magnetic intensity $\mathrm{Re}_x^{1/2}\mathrm{Mg}_x$ and rate of heat transfer $\mathrm{Re}_x^{-1/2}\mathrm{Nu}_x$ on the surface of the plate.

Table 1: Numerical values of $Cf_x Re_x^{1/2}$ obtained for $R_d = 1.0, 10.0$, and $\theta_w = 1.1$ when Pm = 0.1, Pr = 0.1, $\lambda = 1.0$, and $S = 0.1$ against ξ by two methods.

ξ	$R_d = 1.0$		$R_d = 10.0$	
	FDM	Asymptotic	FDM	Asymptotic
0.05	1.62225	1.622809sm	1.55037	1.55809sm
0.1	1.66669	1.66423sm	1.59222	1.59423sm
0.2	1.75771	1.75652sm	1.67797	1.67652sm
0.4	1.94733	1.94108sm	1.85681	1.85108sm
0.8	2.35008	2.350021sm	2.23701	2.23021sm
1.0	2.55973	—	2.43497	—
3.0	4.70172	—	4.45669	—
4.0	5.71434	—	5.41609	—
5.0	6.68702	—	6.34363	—
6.0	7.63595	7.63883Lr	7.25476	7.25883Lr
7.0	8.57192	8.57900Lr	8.15909	8.15900Lr
8.0	9.49946	9.499912Lr	9.06043	9.06912Lr
9.0	10.92063	10.99922Lr	9.96012	9.96174Lr
10.0	11.33623	11.39390Lr	10.85958	10.85930Lr

Table 2: Numerical values of $Mg_x Re_x^{1/2}$ obtained for $R_d = 1.0, 10.0$, and $\theta_w = 1.1$ when Pm = 0.1, Pr = 0.1, $\lambda = 1.0$, and $S = 0.1$ against ξ by two methods.

ξ	$R_d = 1.0$		$R_d = 10.0$	
	FDM	Asymptotic	FDM	Asymptotic
0.05	1.35080	1.35110sm	1.37691	1.37118sm
0.1	1.30772	1.30005sm	1.33024	1.33005sm
0.2	1.22683	1.22780sm	1.24886	1.24780sm
0.4	1.08388	1.08330sm	1.10133	1.10330sm
0.8	0.85853	0.85429sm	0.86924	0.84291sm
1.0	0.76950	—	0.77777	—
3.0	0.32395	—	0.32414	—
4.0	0.23978	—	0.23970	—
5.0	0.18862	—	0.18855	—
6.0	0.15474	0.15667Lr	0.15470	0.215667Lr
7.0	0.13068	0.13286Lr	0.13065	0.13206Lr
8.0	0.11269	0.12500Lr	0.11268	0.11500Lr
9.0	0.09874	0.10111Lr	0.09873	0.11111Lr
10.0	0.08758	0.092741Lr	0.08750	0.081000Lr

4.1. Skin Friction, Magnetic Intensity Coefficient, and Rate of Heat Transfer

In first attempt we have obtained the solution of the nonsimilar boundary layer equations governing the mixed convection flow of a viscous incompressible and electrically conducting fluid along a vertical magnetized porous plate against ξ. Tables 1, 2, and 3 exhibiting the effects of radiation parameter or Planks number $R_d = 1.0, 10.0$ and for the fixed value of buoyancy force parameter $\lambda = 1.0$, magnetic Prandtl number Pm = 0.1 and Prandtl number Pr = 0.1, magnetic force parameter S, and surface temperature $\theta_w = 1.1$ on coefficients

Table 3: Values of $\mathrm{Nu}_x/\mathrm{Re}_x^{1/2}$ against ξ for $R_d = 1.0, 10.0$, and $\theta_w = 1.1$ when $\mathrm{Pm} = 0.1$, $\mathrm{Pr} = 0.1$, $\lambda = 1.0$, and $S = 0.1$ against ξ by two methods.

ξ	$R_d = 1.0$		$R_d = 10.0$	
	FDM	Asymptotic	FDM	Asymptotic
0.05	0.29162	0.29725sm	0.34621	0.34725sm
0.1	0.29321	0.29901sm	0.34935	0.34824sm
0.2	0.29636	0.29954sm	0.35558	0.35654sm
0.4	0.30251	0.30559sm	0.36789	0.36559sm
0.8	0.31429	0.31369sm	0.39189	0.39369sm
1.0	0.31992	—	0.40360	—
3.0	0.37116	—	0.51618	—
4.0	0.39612	—	0.57401	—
5.0	0.42193	—	0.63503	—
6.0	0.44887	0.44860Lr	0.69949	0.69860Lr
7.0	0.47695	0.47170Lr	0.76723	0.76170Lr
8.0	0.50613	0.50480Lr	0.83791	0.83480Lr
9.0	0.53636	0.53790Lr	0.91119	0.91790Lr
10.0	0.56757	0.563100Lr	0.98672	0.98310Lr

sm stand for small ξ, where Lr for large ξ.

of skin friction $\mathrm{Re}_x^{1/2}\mathrm{Cf}_x$, rate of heat transfer $\mathrm{Re}_x^{-1/2}\mathrm{Nu}_x$ and magnetic intensity $\mathrm{Re}_x^{1/2}\mathrm{Mg}_x$ at the surface. From Tables 1, 2, and 3, it can easily be seen that an increase in radiation parameter R_d leads to decrease in coefficient of local skin friction and increases in the rate of heat transfer, magnetic intensity at the surface. This phenomenon can easily be understood from the fact that when radiation parameter R_d increases, the ambient fluid temperature decreases and Roseland mean absorption coefficient increases which reduce the skin friction and enhance the rate of heat transfer and magnetic intensity at the surface. In Figures 2(a), 2(b), and 2(c), where it is observed that with the increase of radiation parameter R_d the skin friction decreases and rate of heat transfer and magnetic intensity at the surface increases. In Figures 3(a), 3(b), and 3(c) it can be seen that the increase in buoyancy force parameter $\lambda = 0.0, 2.5, 5.0, 7.5, 10$ the coefficient of skin friction, heat transfer increases and magnetic intensity at the surface decreases. It is very interesting fact that forced convection is dominant mode of flow and heat transfer when buoyancy parameter $\lambda \rightarrow 0$ but with the increase of λ the buoyancy force acts like pressure gradient and increase the the fluid motion, hence the coefficients of skin friction, heat transfer and magnetic intensity increases with the streamwise distance ξ.

Figures 4(a), 4(b), and 4(c) are representing the effects of different values of Prandtl number $\mathrm{Pr} = 0.01, 0.1, 0.71, 7.0$, and for fixed value of buoyancy force parameter $\lambda = 1.0$, magnetic field parameter $S = 0.4$ and magnetic Prandtl number $\mathrm{Pm} = 0.1$, radiation parameter $R_d = 1.0$, surface temperature $\theta_w = 1.1$, on the coefficients of skin friction, rate of heat transfer and magnetic intensity at the surface. In these figures, it is observed that with increase of Prandtl number Pr the coefficient of skin friction decreases, coefficient of heat transfer and magnetic intensity at the surface increases. It is very pertinent to mention that the increase in the Prandtl number Pr increases the kinematic viscosity (which ratio of dynamic viscosity to density of the fluid) of the fluid and decreases the thermal diffusion which causes the increase in momentum boundary layer thickness and due to rise in temperature thermal boundary layer becomes thinner. So, these factors are responsible for the aforementioned

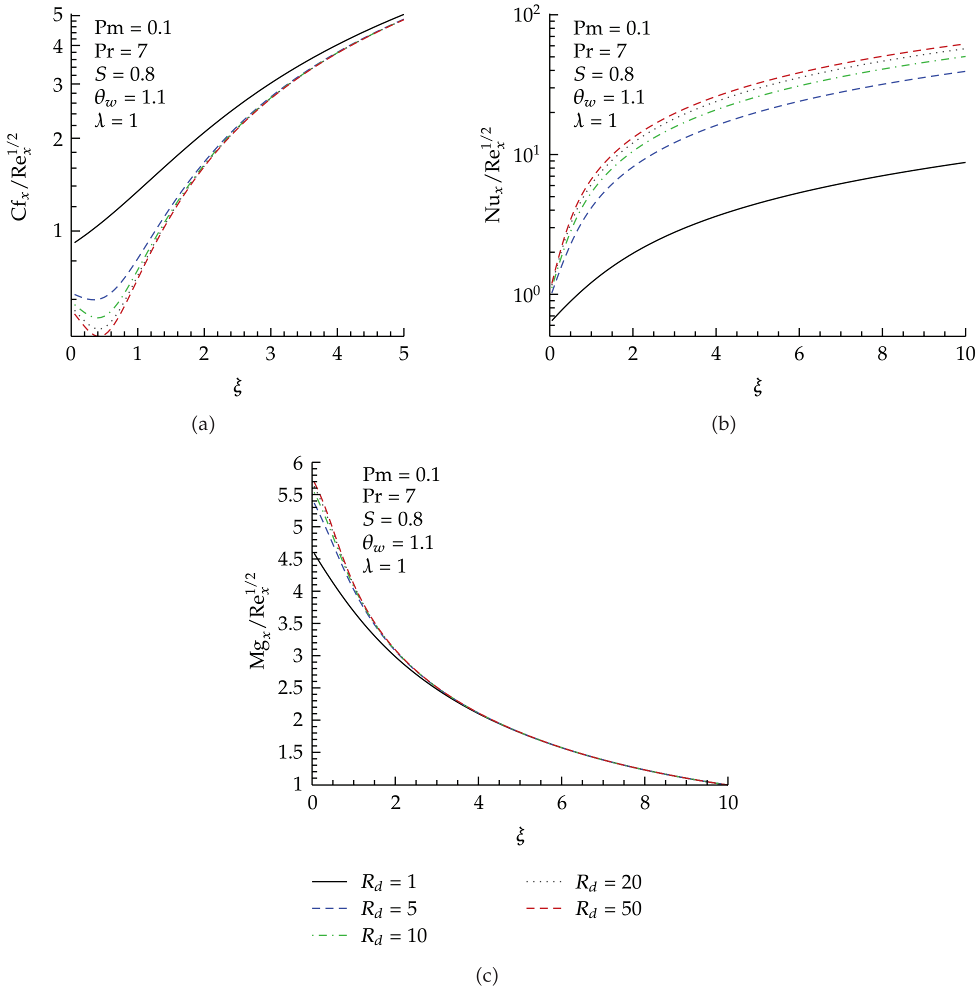

Figure 2: Numerical solution of (a) skin friction coefficient and (b) coefficient of rate of heat transfer (c) coefficient of magnetic intensity at the surface against ξ for different values of radiation parameter $R_d = 1.0, 5.0, 10.0, 20.0, 50.0$, $\mathrm{Pm} = 0.1$, $\mathrm{Pr} = 7.0$, and $S = 0.8$, $\theta_w = 1.1$, $\lambda = 1.0$.

phenomena. In Figures 5(a), 5(b), and 5(c) the effects of different values of magnetic Prandtl number Pm by keeping other parameters fixed on coefficients of skin friction, heat transfer and magnetic intensity are displayed. From these figures it is shown that the increase in magnetic Prandtl number $\mathrm{Pm} = 1.0, 10.0, 100.0$ increase the coefficients of skin friction, heat transfer and decrease the coefficient of magnetic intensity at the surface. It is also noted that the increase in coefficients of skin friction, heat transfer very remarkable for large values of magnetic Prandtl Pm, that is, for $\mathrm{Pm} = 10.0$, 100.0 as compared with magnetic intensity at the surface. The reason is that with the increase of magnetic Prandtl number Pm the magnetic diffusion γ decreases or product of magnetic permeability, electrical conductivity and kinematic viscosity at the surface increases and hence the momentum and thermal boundary layer thicknesses decreases due to which coefficients of skin friction and heat transfer increases and magnetic intensity at the surface decreases.

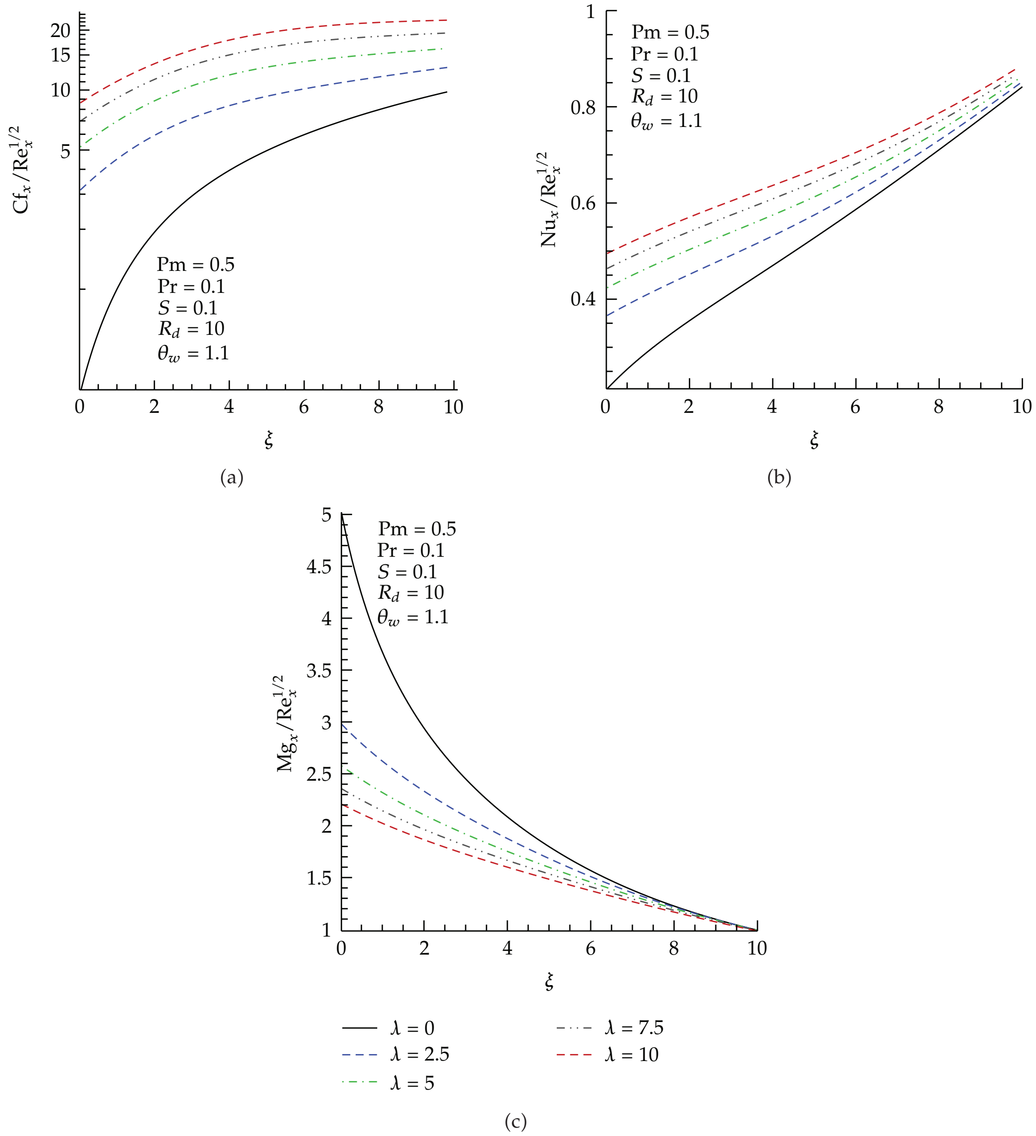

Figure 3: Numerical solution of (a) skin friction coefficient and (b) coefficient of rate of heat transfer (c) coefficient of magnetic intensity at the surface against ξ for different values of mixed convection parameter $\lambda = 0.0, 2.5, 5.0, 7.5, 10.0$ when Pm $= 0.5$, Pr $= 0.1$, $S = 0.1$, $R_d = 10.0$, and $\theta_w = 1.1$.

4.2. Velocity, Temperature and Magnetic Profiles

Now we will discuss the effects of different physical parameters on the profiles of the velocity, temperature and the transverse component of magnetic field against similarity variable η for transpiration parameter $\xi = 10.0$. The effects of mixed convection parameter $\lambda = 0.0, 2.5, 5.0, 7.5, 10.0$, for two values of magnetic field parameter $S = 0.0, 0.8$ and for fixed value of magnetic Prandtl number Pm $= 1.6$, Pr $= 0.1$, $\xi = 0.5$, radiation parameter $R_d = 10.0$, and surface temperature $\theta_w = 1.1$ on velocity, temperature and transverse component of magnetic field profiles are shown in Figures 6(a), 6(b), and 6(c). The dotted and solid lines in

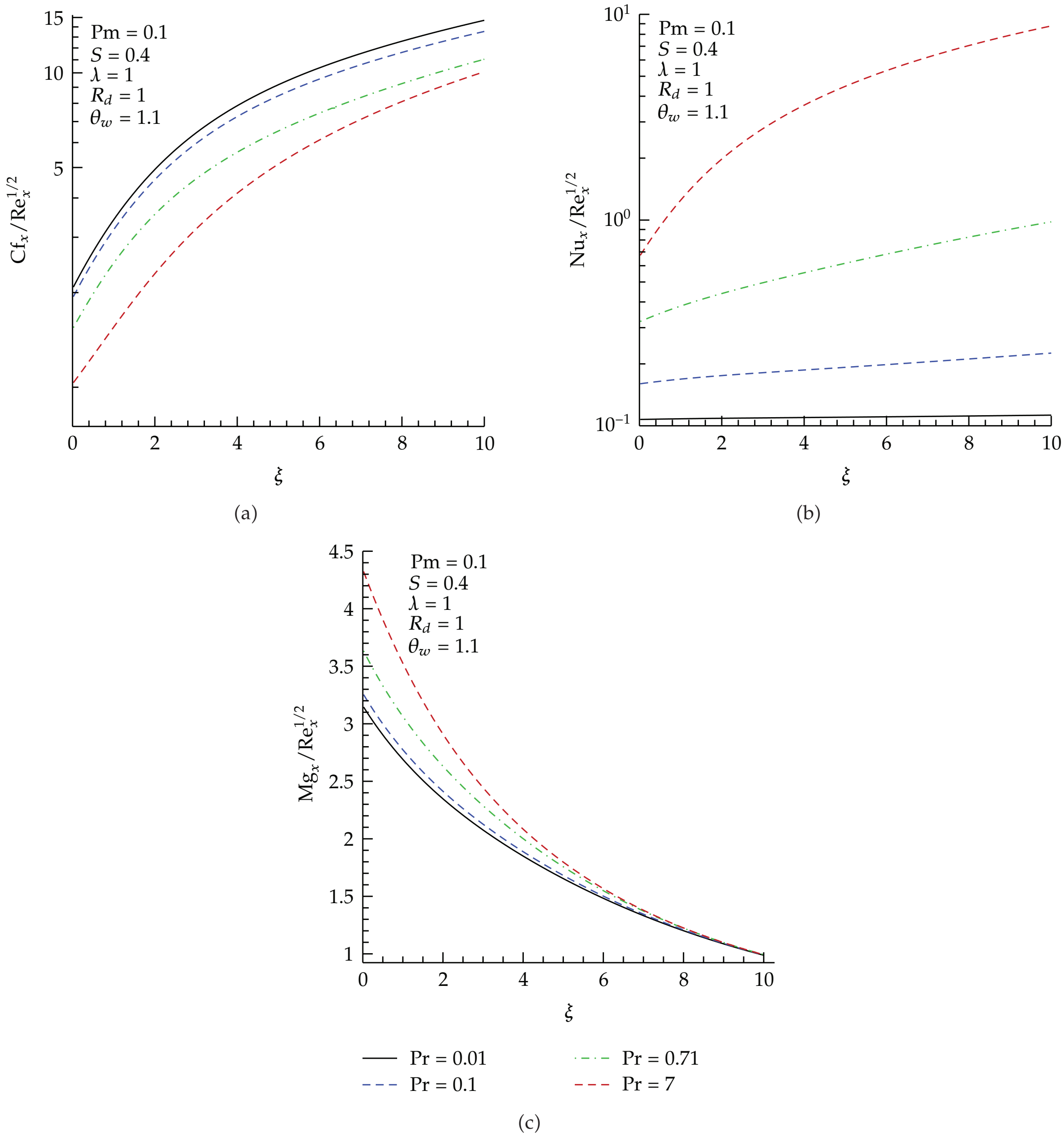

Figure 4: Numerical solution of (a) skin friction coefficient and (b) coefficient of rate of heat transfer (c) coefficient of magnetic intensity at the surface against ξ for different values of Prandtl number $Pr = 0.01, 0.1, 0.71, 7.0$ when $Pm = 0.1$, $S = 0.4$, $R_d = 1.0$, $\theta_w = 1.1$ and $\lambda = 1.0$.

Figures 6(a)–6(c) shown the effects of parameter λ for $S = 0$ (absence of magnetic field) and $S = 0.8$ (presence of magnetic field), respectively. It is concluded that the velocity profile is influenced considerably and increase when the value of λ increases and there is no any significant changes shows in the absence of magnetic field as shown by dotted lines in Figure 5(a). In Figure 6(b) it is shown that the temperature decreases with the increase of λ and there is no changes seen for magnetic field parameter $S = 0$ and $S = 0.8$. From Figure 6(c), we note that with the increase of parameter λ the effects of transverse component of magnetic field decreases against η.

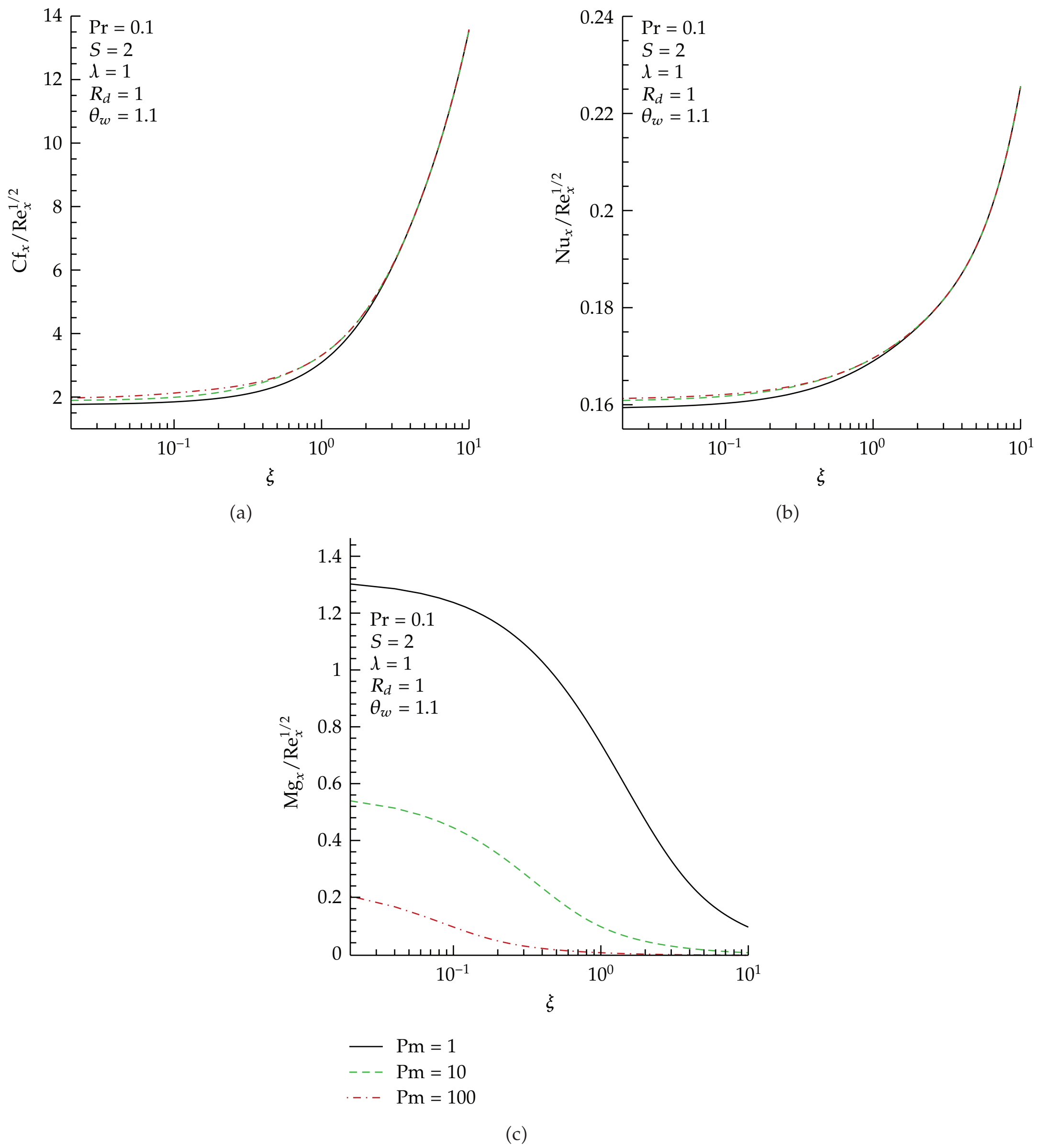

Figure 5: Numerical solution of (a) skin friction coefficient and (b) coefficient of rate of heat transfer (c) coefficient of magnetic intensity at the surface against ξ for different values of magnetic Prandtl number $\mathrm{Pm} = 1.0, 10.0, 100.0$ when $\mathrm{Pr} = 0.1$, $S = 2.0$, $R_d = 1.0$, $\theta_w = 1.1$, and $\lambda = 1.0$.

Figures 7(a), 7(b), and 7(c) are based on the effects of the magnetic field parameter S on the velocity, temperature and component of transverse magnetic field profiles. These figures clearly show that with the increase of magnetic force parameter S the velocity profile decreases and the temperature, transverse component of magnetic field profile increases. In Figures 8(a), 8(b), and 8(c) it is noted that the increase in transpiration parameter ξ increase velocity profile and decrease the temperature and transverse component of magnetic field profiles. From these figures it is also concluded that the momentum boundary layer thickness decreases and thermal boundary layer thickness increases which indicates that transpiration destabilizes the boundary layer. Finally, in Figures 9(a), 9(b), and 9(c) it is shown that with the increase of radiation parameter R_d and keeping other parameters fixed the velocity and temperature distribution decreases and transverse component of magnetic field increases.

4.3. Asymptotic Solutions for Small and Large ξ

Now we are heading in finding the solution of the present problem for small and large value of transpiration parameter ξ. To do this we first reduce the equations (2.1)–(2.7) to convenient form by introducing the following transformations:

$$\psi = x^{1/2}\left[f(\eta,\xi) + \xi\right],$$
$$\varphi = x^{-1/2}\phi(\eta,\xi), \qquad \overline{\theta} = x^{-1}\theta(\eta,\xi), \tag{4.1}$$
$$\eta = x^{-1/2}, \qquad \xi = sx^{1/2},$$

where, η is the similarity variable, ξ be the local transpiration parameter and ψ, ϕ are the function which satisfy the equations of conservation of mass and magnetic field such that:

$$u = \frac{\partial\psi}{\partial y}, \qquad v = -\frac{\partial\psi}{\partial x}, \qquad H_x = \frac{\partial\varphi}{\partial y}, \qquad H_y = -\frac{\partial\varphi}{\partial x}. \tag{4.2}$$

For withdrawal of fluid $\xi > 0$ whereas for blowing of fluid through the surface of the plate $\xi < 0$. Throughout the present computations, value of ξ has been considered positive.

By using (4.1) and (4.2) in (2.1)–(2.15), we will obtain the following dimensionless local nonsimilarity equations:

$$f''' + \frac{1}{2}(ff'' - S\phi\phi'') + \xi f'' + \lambda\theta = \frac{1}{2}\xi\left[f'\frac{\partial f'}{\partial\xi} - f''\frac{\partial f}{\partial\xi} - S\left(\phi'\frac{\partial\phi'}{\partial\xi} - \phi''\frac{\partial\phi}{\partial\xi}\right)\right], \tag{4.3}$$

$$\frac{1}{\mathrm{Pm}}\phi'' + \frac{1}{2}(f\phi' - f'\phi) + \xi\phi' = \frac{1}{2}\xi\left[f'\frac{\partial\phi}{\partial\xi} - \phi'\frac{\partial f}{\partial\xi}\right], \tag{4.4}$$

$$\frac{1}{\mathrm{Pr}}\left[1 + \frac{4}{3R_d}(1+\Delta\theta)^3\right]\theta'' + \frac{1}{2}f\theta' + f'\theta + \xi\theta' = \frac{1}{2}\xi\left[f'\frac{\partial\theta}{\partial\xi} - \theta'\frac{\partial f}{\partial\xi}\right], \tag{4.5}$$

where, $S = \overline{\mu}H_0^2/\rho U_0^2$, $\mathrm{Pm} = v/\gamma$, respectively, are known as magnetic field parameter and magnetic Prandtl number and $\Delta = \theta_w - 1$. The corresponding boundary conditions becomes

$$f(0,\xi) = 0, \qquad f'(0,\xi) = 0, \qquad \phi'(0,\xi) = 1, \qquad \theta(0,\xi) = 1,$$
$$f'(\infty,\xi) = 1, \qquad \phi'(\infty,\xi) = 0, \qquad \theta(\infty,\xi) = 0. \tag{4.6}$$

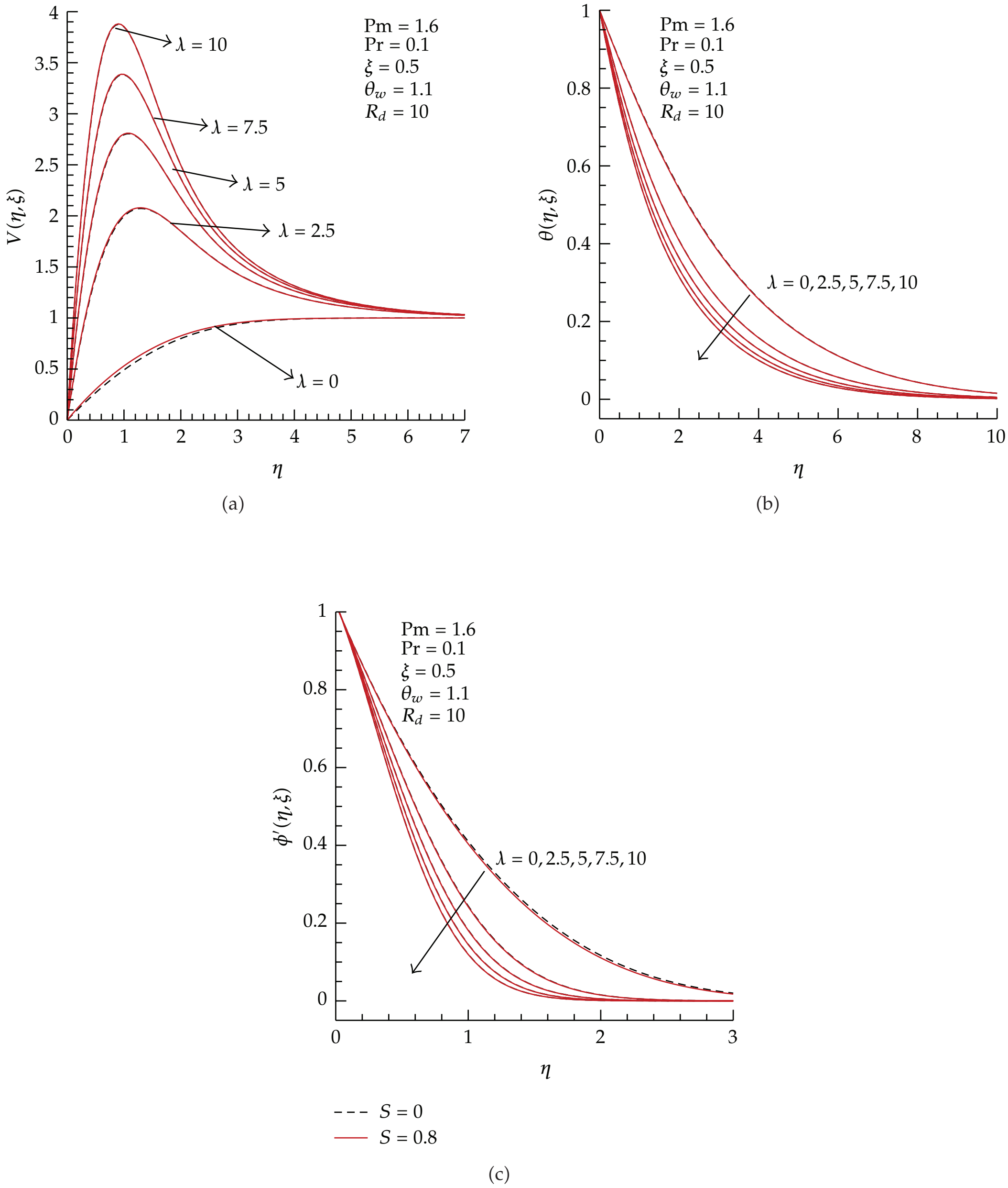

Figure 6: (a) velocity and (b) temperature (c) transverse component of magnetic field profile against η at $\xi = 0.5$ for different values of mixed convection parameter $\lambda = 0.0, 2.5, 5.0, 7.5, 10.0$ when $S = 0.0, 0.8$ and for $\mathrm{Pr} = 0.1$, and $\mathrm{Pm} = 1.6$, $R_d = 10.0$, $\theta_w = 1.1$.

It can be seen from equations (4.3)–(4.5) that for $\xi = 0.0$, the set of equations become similar by nature, solutions of which can easily be obtained by standard shooting method, otherwise these equations are locally nonsimilar, solution methodology of which will be discussed in the following sections. Once we know the solution of these equations, physical quantities of interest such as, the skin-friction coefficient, Cf_x, and the magnetic intensity Mg_x, and the rate of heat transfer Nu_x at the surface may be calculated from

$$\begin{aligned}
\mathrm{Re}_x^{1/2}\mathrm{Cf}_x &= f''(\xi,0),\\
\mathrm{Re}_x^{1/2}\mathrm{Mg}_x &= -\phi(\xi,0),\\
\mathrm{Re}_x^{-1/2}\mathrm{Nu}_x &= -\left(1+\frac{4}{3R_d}\right)\theta'(\xi,0).
\end{aligned} \tag{4.7}$$

4.3.1. Solution for Small ξ

Since near the leading edge ξ is small ($\xi \ll 1$), solutions to the equations (4.3)–(4.5) with boundary conditions (4.6) may be obtained by using the perturbation method. We can expand all the depending functions in powers of ξ, we consider that

$$f(\xi,\eta) = \sum_{i}^{\infty}\xi^i f_i(\eta), \qquad \phi(\xi,\eta) = \sum_{i=0}^{\infty}\xi^i\phi_i(\eta), \qquad \theta(\xi,\eta) = \sum_{i=0}^{\infty}\xi^i\theta_i(\eta). \tag{4.8}$$

Substituting (4.8) into expression (4.3)–(4.5), and taking the terms only up to $O(\xi^2)$ we will get the system of equations together with boundary conditions (4.6) which is given as follows:

$$\begin{gathered}
f_0''' + \frac{1}{2}\left(f_0 f_0'' - S\phi_0\phi_0''\right) + \lambda\theta_0 = 0,\\
\frac{1}{\mathrm{Pm}}\phi_0'' + \frac{1}{2}\left(f_0\phi_0' - \phi_0 f_0'\right) = 0,\\
\left[1+\alpha(1+\Delta\theta_0)^3\right]\theta_0'' + 3\alpha\Delta(1+\Delta\theta_0)^2\theta_0'^2 + \frac{\mathrm{Pr}}{2}f_0\theta_0' + \mathrm{Pr} f_0'\theta_0 = 0,\\
f_0(0,\xi) = 0, \qquad f_0'(0,\xi) = 0, \qquad \phi_0'(0,\xi) = 1, \qquad \theta_0(0,\xi) = 1,\\
f_0'(\infty,\xi) = 1, \qquad \phi_0'(\infty,\xi) = 0, \qquad \theta_0(\infty,\xi) = 0,\\
f_1''' + \frac{1}{2}\left(f_0 f_1'' - f_0' f_1' - S\left(\phi_0\phi_1'' - \phi_0'\phi_1'\right)\right) + \left(f_0'' f_1 - S\phi_0''\phi_1\right) + f_0'' + \lambda\theta_1 = 0,\\
\frac{1}{\mathrm{Pm}}\phi_1'' + \frac{1}{2}\left(f_0\phi_1' - f_1'\phi_0\right) + \left(f_0'\phi_1 - f_1\phi_0'\right) + \phi_0' = 0,
\end{gathered}$$

$$
\begin{aligned}
&\left[1+\alpha(1+\Delta\theta_0)^3\right]\theta_1''+3\alpha\Delta(1+\Delta\theta_0)^2\left(\theta_1\theta_0''+2\theta_0'\theta_1'\right)\\
&\quad+6\alpha\Delta^2\theta_1(1+\Delta\theta_0)\theta_0'^2+\frac{\Pr}{2}\left(f_0\theta_1'+f_0'\theta_1\right)+\Pr\left(f_1\theta_0'+\theta_0f_1'\right)+\Pr\theta_0'=0,\\
&\quad f_1(0,\xi)=0,\qquad f_1'(0,\xi)=0,\qquad \phi_1'(0,\xi)=0,\qquad \theta_1(0,\xi)=0,\\
&\quad f_1'(\infty,\xi)=0,\qquad \phi_1'(\infty,\xi)=0,\qquad \theta_1(\infty,\xi)=0,\\
&f_2'''+\frac{1}{2}\left(f_0f_2''-f_1'^2-S\left(\phi_0\phi_2''-\phi_1'^2\right)\right)+\left(f_1f_1''-f_0'f_2'-S(\phi_1\phi_1''-\phi_0'\phi_2')\right)\\
&\quad+\frac{3}{2}\left(f_0''f_2-S\phi_0''\phi_2\right)+f_1''+\lambda\theta_2=0,\\
&\frac{1}{\mathrm{Pm}}\phi_2''+\frac{1}{2}\left(f_0\phi_2'-f_0'\phi_2\right)+\left(f_1\phi_1'-f_1'\phi_1\right)+\frac{3}{2}\left(\phi_0'f_2-f_0'\phi_2\right)+\phi_1'=0,\\
&\left[1+\alpha(1+\Delta\theta_0)^3\right]\theta_2''+3\alpha\Delta\theta_1''\theta_1(1+\Delta\theta_0)^2\\
&\quad+3\alpha\Delta\theta_0''\left[\theta_2''+\Delta\left(2\theta_2\theta_0+\theta_1^2\right)+\Delta^2\theta_0\left(\theta_2\theta_0+\theta_1^2\right)\right]\\
&\quad+3\alpha\Delta\left[\left(2\theta_2'\theta_0'+\theta_1^2\right)(1+\Delta\theta_0)^2+4\Delta\theta_1'\theta_1\theta_0(1+\Delta\theta_0)+\Delta\theta_0^2\left(2\theta_2+\Delta\left(2\theta_2\theta_0+\theta_1^2\right)\right)\right]\\
&\quad+\frac{\Pr}{2}\left(f_0\theta_2'+\theta_1f_1'\right)+\left(\theta_1'f_1+f_2'\theta_0\right)+\frac{3\Pr}{2}f_2\theta_0'+\Pr\theta_1'=0,\\
&\quad f_2(0,\xi)=0,\qquad f_2'(0,\xi)=0,\qquad \phi_2'(0,\xi)=0,\qquad \theta_2(0,\xi)=0,\\
&\quad f_2'(\infty,\xi)=0,\qquad \phi_2'(\infty,\xi)=0,\qquad \theta_2(\infty,\xi)=0.
\end{aligned}
\tag{4.9}
$$

It is pertinent to mentioned that (4.9) are coupled and nonlinear, so the solutions of these equations can be obtained by the Nachtsheim-Swigert iteration technique together with the sixth-order implicit Runge-Kutta-Butcher initial value solver. After knowing the values of the functions f'', ϕ and θ' and their derivatives we can calculate the values of the coefficient of skin friction, surface magnetic intensity and heat transfer in the region near the leading edge against ξ from the following expansion for $S = 0.1$, $\lambda = 1.0$, $\mathrm{Pm} = 0.1$, $\Pr = 0.1$, and radiation parameter $R_d = 1.0, 10.0$, and $\theta_w = 1.1$, respectively.

$$
\begin{aligned}
\mathrm{Re}_x^{1/2}\mathrm{Cf}_x &= \left(1.59195+1.12282\xi+1.01047\xi^2+\cdots\right),\\
\mathrm{Re}_x^{1/2}\mathrm{Mg}_x &= -\left(1.43230+1.02251\xi+1.34209\xi^2+\cdots\right),\\
\mathrm{Re}_x^{-1/2}\mathrm{Nu}_x &= -\left(0.21749-0.00475\xi+0.09878\xi^2\cdots\right).
\end{aligned}
\tag{4.10}
$$

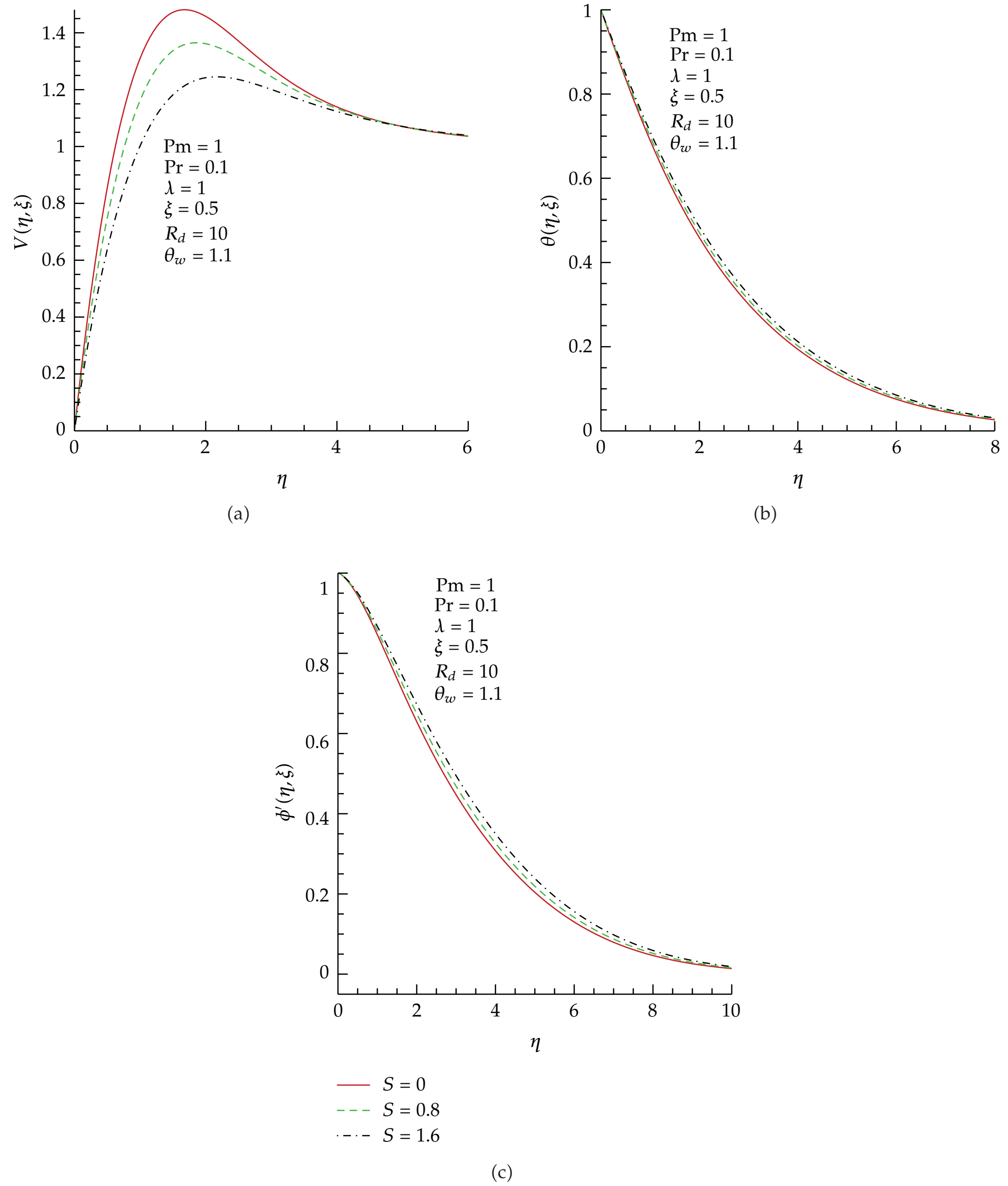

Figure 7: (a) velocity and (b) temperature (c) transverse component of magnetic field profile against η at $\xi = 0.5$ for different values magnetic field parameter $S = 0.0, 0.8, 1.6$ when $\lambda = 1.0$ and for $\mathrm{Pr} = 0.1$, and $\mathrm{Pm} = 1.0$, $R_d = 10.0$, $\theta_w = 1.1$.

The numerical results thus obtained or entered in Tables 1, 2, and 3 for coefficients of skin friction, rate of heat transfer and magnetic intensity at the surface. We can see that from these tables the series solution are in excellent agreement with that of finite difference solutions even for $\xi \, \varepsilon [0, 1]$.

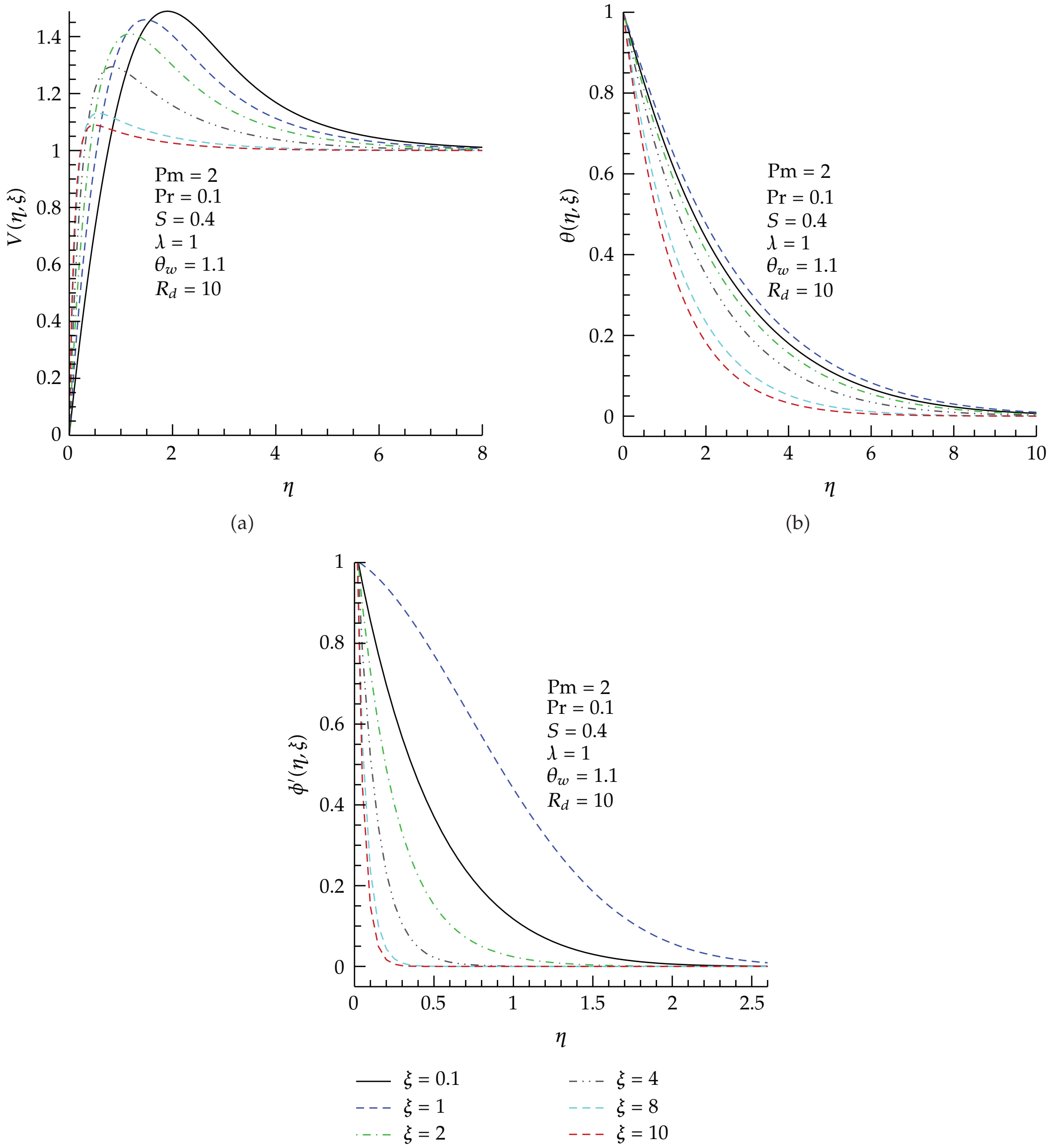

(c)

Figure 8: (a) velocity and (b) temperature (c) transverse component of magnetic field profile against η for different values transpiration parameter $\xi = 2.0, 1.0, 2.0, 4.0, 8.0, 10.0$, when $S = 0.4$, $\lambda = 1.0$, and for $\mathrm{Pr} = 0.1$, $\mathrm{Pm} = 2.0$, $R_d = 10.0$, θ_w=1.1

In Table 4 the comparison of the solutions obtained by finite difference method and that of Glauert [11] analytically has been given for the coefficient of skin friction and magnetic intensity at the surface. It is observed that for $\mathrm{Pm} = 1.0, 10.0$, radiation parameter $R_d = \infty$, and the variation in magnetic field parameter S decrease the skin friction and the skin friction approaches to zero as $S \rightarrow 1.1$ and the local magnetic intensity Mg_x increases with the increase of magnetic field parameter S. From this table it can be seen that the present method and the analytical results obtained by Glauert [11] are in good agreement.

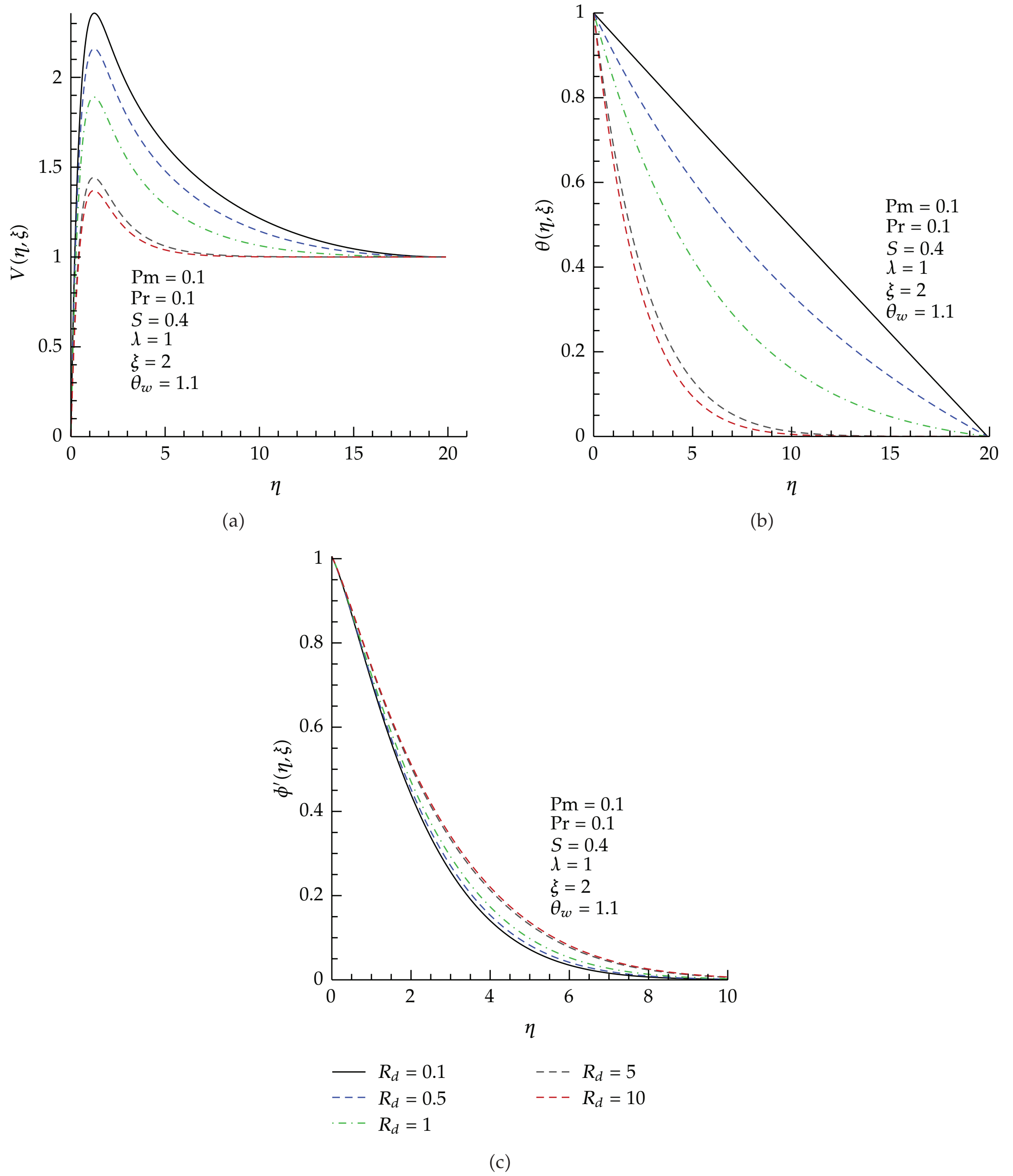

Figure 9: (a) velocity and (b) temperature (c) transverse component of magnetic field profile against η for different values radiation parameter $R_d = 0.1, 0.5, 1.0, 5.0, 10.0$ when $S = 0.4$, $\lambda = 1.0$ and for $\xi = 2.0$, $\text{Pr} = 0.1$, $\text{Pm} = 0.1$, $\theta_w = 1.1$.

For magnetic Prandtl number $\text{Pm} = 10.0$ the coefficients of skin friction and magnetic intensity at the surface are also noted in excellent agreement. Further, we see that for small value of magnetic Prandtl number $\text{Pm} = 0.1$, and for magnetic field parameter $S = \pi$ as in the case of Glauert [11] the separation occur at the surface. In Table 5 the value of coefficient of skin friction obtained by other authors Glauert [11] for large magnetic Prandtl

Table 4: Values of $\mathrm{Re}_x^{1/2}\mathrm{Cf}_x$ and $\mathrm{Re}_x^{1/2}\mathrm{Mg}_x$ obtained by Glauert [2] and present authors while $R_d = \infty$, Pm = 1.0 and 10.0 against different values of S.

S	Pm = 1.0				Pm = 10.0			
	Present		Glauret [2]		Present		Glauret [2]	
	$f''(0)$	$g(0)$	$f''(0)$	$g(0)$	$f''(0)$	$g(0)$	$f''(0)$	$g(0)$
0.0	0.3321	2.1290	0.3321	2.1797	0.3321	0.9525	0.3321	1.0095
0.1	0.3067	2.1713	0.3025	2.2448	0.3188	0.9631	0.3182	1.0238
0.2	0.2806	2.2191	0.2729	2.3099	0.3050	0.9744	0.3044	1.0380
0.4	0.2257	2.3372	0.2138	2.4402	0.2770	0.9995	0.2767	1.0665
0.6	0.1657	2.5066	0.1547	2.5704	0.2479	1.0285	0.2491	1.0950
0.8	0.0972	2.8017	0.0955	2.7006	0.2176	1.0629	0.2214	1.1235
1.0	0.0014	4.8488	0.0364	2.8308	0.1857	1.1051	0.1938	1.1520
1.1	0.0000	6.0423	0.0068	2.8959	0.1691	1.1302	0.1799	1.1662

Table 5: Values of $\mathrm{Re}_x^{1/2}\mathrm{Cf}_x$ when $R_d = \infty$, $S =$ 0.1 and 0.05 at $\xi = 0.0$ against Pm obtain by Glauert [2] and Devies [3] and the present authors.

Pm	$s = 0.0$ Present	Glauert [2]	Pm	$s = 0.8$ Present	Davies [3]
0.1	0.2888	0.2669	0.1	0.3106	0.3140
1.0	0.3067	0.3016	0.2	0.3107	0.3157
2.0	0.3109	0.3078	0.3	0.3153	0.3173
4.0	0.3145	0.3128	0.5	0.3172	0.3194
6.0	0.3164	0.3152	0.7	0.3183	0.3204
8.0	0.3177	0.3167	0.9	0.3191	0.3204
10.0	0.3186	0.3178	—	—	—
—	—	—	—	—	—
50	0.3238	0.3237	—	—	—
75	0.3248	0.3247	—	—	—
100	0.3254	0.3254	—	—	—

number Pm by keeping $R_d = \infty$ and Davies [2] for small magnetic Prandtl number by taking magnetic field parameter $S = 0.1$ and sufficiently small $S = 0.05$ are entered and compare with present results and found to be in good agreement. Here we notice that the agreement between present results and results obtained by Glauert [11], Davies [2] are in excellent agreement. The results entered in Table 6 are those obtained from heat transfer in hydromagnetics by Ramamoorthy [6] considering Eckert number equal to zero and radiation parameter $R_d = \infty$are compared with the present results. From this table it can be seen that the numerical results obtained for different values of magnetic field parameter S and for $\mathrm{Pm} = 0.1$, $\mathrm{Pr} = 1.0$, $\lambda = 0.5$ are very closed the results obtained by Ramamoorthy.

Table 6: Values of $\mathrm{Re}_x^{-1/2}\mathrm{Nu}_x$ for different S when $R_d = \infty$, Pm = 0.1, Pr = 1.0, and $\lambda = 0.5$ obtained by present authors and Ramamoorthy [6].

S	Present	[6]
0.1	0.64551	0.65048
0.3	0.61994	0.61958
0.5	0.59112	0.57693

4.3.2. Solution for Large ξ

Now, attention is given in finding the solution of equations (4.3)–(4.6) when ξ is large. The order of magnitude analysis of various terms in these equations shows that f''' and $\xi f''$ are largest terms in (4.3) and ϕ'' and $\xi\phi'$ in (3.14) and θ'' and $\xi\theta'$ in (4.5). In the respective equations, both the terms have to be balanced in magnitude and the only way to do this, is to assume that η is small and hence its derivative is large. It is essential to find appropriate scaling for f, ϕ and θ. On balancing f''' and $\xi f''$ in (4.3) and ϕ'' and $\xi\phi'$ in (4.4) and θ'', $\xi\theta'$ in (4.5), it is found that $\eta = O(\xi^{-1})$, $f = O(\xi^{-1})$, and $\phi = O(\xi^{-1})$. Therefore, following transformations may be introduced

$$f(\eta) = \xi^{-1}\overline{f}(\overline{\eta}), \qquad \overline{\eta} = \xi\eta, \qquad \phi(\eta) = \xi^{-1}\overline{\phi}(\overline{\eta}), \qquad \theta(\eta) = \overline{\theta}(\overline{\eta}). \tag{4.11}$$

By using (4.10), the transformed equation will take the form:

$$\overline{f}''' + \overline{f}'' + \lambda\xi^{-2}\theta = \frac{1}{2f}\left[\overline{f}'\frac{\partial \overline{f}}{\partial \xi} - \overline{f}''\frac{\partial \overline{f}}{\partial \xi} - S\left(\overline{\phi}'\frac{\partial \overline{\phi}'}{\partial \xi} - \overline{\phi}''\frac{\partial \overline{\phi}}{\partial \xi}\right)\right], \tag{4.12}$$

$$\frac{1}{\mathrm{Pm}}\overline{\phi}'' + \overline{\phi}' = \frac{1}{2}\xi^{-1}\left[\overline{f}'\frac{\partial \overline{\phi}}{\partial \xi} - \overline{f}'\frac{\partial \overline{f}}{\partial \xi}\right], \tag{4.13}$$

$$\frac{1}{\mathrm{Pr}}\left[1 + \frac{4}{3R_d}(1+\Delta\theta)^3\right] + \overline{\theta}' = \frac{1}{2}\xi^{-1}\left[\overline{f}'\frac{\partial \overline{\theta}}{\partial \xi} - \overline{\theta}'\frac{\partial \overline{f}}{\partial \xi}\right]. \tag{4.14}$$

The regular perturbation of the functions $\overline{f}$, $\overline{\phi}$ and $\overline{\theta}$ in power of ξ^{-2} is given as follows:

$$\overline{f}(\xi,\overline{\eta}) = \sum_{m=0}^{1}\xi^{-2m}\overline{f}_m(\overline{\eta}), \qquad \overline{\phi}(\xi,\overline{\eta}) = \sum_{m=0}^{1}\xi^{-2m}\overline{\phi}_m(\overline{\eta}), \qquad \overline{\theta}(\xi,\overline{\eta}) = \sum_{m=0}^{1}\xi^{-2m}\overline{\theta}_m(\overline{\eta}). \tag{4.15}$$

By substituting (4.14) into (4.11)–(4.13), and equating like power of ξ and by dropping bars we have the following set of equations:

$O(\xi^0)$:

$$
\begin{gathered}
f_0''' + f_0'' = 0, \\
\frac{1}{\mathrm{Pm}}\phi_0'' + \phi_0' = 0, \\
\left[1+\alpha(1+\Delta\theta_0)^3\right]\theta_0'' + 3\alpha\Delta(1+\Delta\theta_0)^2\theta_0'^2 + \mathrm{Pr}\theta_0' = 0.
\end{gathered} \tag{4.16}
$$

The boundary conditions regarding to the perturbation series expansion are of the following form:

$$
\begin{gathered}
f_0(0) = 0, \qquad f_0'(0) = 0, \qquad \phi_0'(0) = 1, \qquad \theta_0(0) = 1, \\
f_0'(\infty) = 1, \qquad \phi_0'(\infty) = 0, \qquad \theta_0(\infty) = 0.
\end{gathered} \tag{4.17}
$$

$O(\xi^{-2})$:

$$
\begin{gathered}
f_1''' + f_1'' + \lambda\theta_0 = 0, \\
\frac{1}{\mathrm{Pm}}\phi_1'' + \phi_1' = 0, \\
\left[1+\alpha(1+\Delta\theta_0)^3\right]\theta_1'' + 3\alpha\Delta(1+\Delta\theta_0)^2\left(\theta_1\theta_0'' + 2\theta_0'\theta_1'\right) + 6\alpha\Delta^2\theta_1(1+\Delta\theta_0)\theta_0'^2 + \mathrm{Pr}\theta_1' = 0.
\end{gathered} \tag{4.18}
$$

And the boundary conditions regarding to the perturbation series expansion are of the following form:

$$
\begin{gathered}
f_1(0) = 0, \qquad f_1'(0) = 0, \qquad \phi_1'(0) = 0, \qquad \theta_1(0) = 0, \\
f_1'(\infty) = 0, \qquad \phi_1'(\infty) = 0, \qquad \theta_1(\infty) = 0.
\end{gathered} \tag{4.19}
$$

From the solutions of (4.15)–(4.16) and (4.17)–(4.18), we obtain

$$
\begin{gathered}
f_0(\eta) = \eta + e^{-\eta} - 1, \\
f_0''(0) = 1, \\
\phi_0(\eta) = -\frac{1}{\mathrm{Pm}}e^{-\eta\mathrm{Pm}},
\end{gathered}
$$

$$\begin{aligned}
\phi_0(0) &= -\frac{1}{\text{Pm}},\\
\theta_0'(\eta) &= \left[1+\frac{4}{3R_d}(1+\Delta\theta_0)^3\right]\text{Pr}e^{-\eta\text{Pr}},\\
\theta_0'(0) &= \left[1+\frac{4}{3R_d}(1+\Delta\theta_0)^3\right]\text{Pr},\\
f_1''(\eta) &= \frac{\lambda e^{-\eta\text{Pr}}(\text{Pr}-1)+\text{Pr}\lambda e^{-\eta}-\lambda e^{-\eta}}{2(\text{Pr}-1)},\\
f_1''(0) &= \frac{\lambda(\text{Pr}-1)+\text{Pr}\lambda-\lambda}{2(\text{Pr}-1)},\\
\phi_1(\eta) &= 0,\\
\phi_1(0) &= 0,\\
\theta_1'(\eta) &= 0,\\
\theta_1'(0) &= 0.
\end{aligned} \tag{4.20}$$

Since, now, we know the values of $f_0''(0)$, $\phi_0(0)$, and $\theta_0'(0)$, and $f_1''(0)$, $\phi_1(0)$, and $\theta_1'(0)$ from the above solutions we calculate the friction coefficient, $\text{Re}_x^{1/2}\text{Cf}_x$, local rate of heat transfer, $\text{Re}_x^{-1/2}\text{Nu}_x$, and the local magnetic intensity, $\text{Re}_x^{1/2}\text{Mg}_x$ at the surface from the following expressions:

$$\begin{aligned}
\text{Re}_x^{1/2}\text{Cf}_x &\simeq \xi+\frac{\lambda(\text{Pr}-1)+\text{Pr}\lambda-\lambda}{2(\text{Pr}-1)}\xi^{-1},\\
\text{Re}_x^{1/2}\text{Mg}_x &\simeq \frac{\xi}{\text{Pm}},\\
\text{Re}_x^{-1/2}\text{Nu}_x &\simeq \left[1+\frac{4}{3R_d}(1+\Delta\theta_0)^3\right]\text{Pr}\xi.
\end{aligned} \tag{4.21}$$

Numerical value of the local skin friction coefficient, surface magnetic intensity and the local rate of heat transfer are obtained from the relations (4.21) for different values of magnetic field parameter S and magnetic Prandtl number Pm and radiation parameter R_d, and surface temperature θ_w, Prandtl number Pr, respectively, in the down stream region are entered in Tables 1, 2, and 3, respectively. From these tables it can be seen that for large value of transpiration parameter ξ the skin friction $\text{Re}_x^{1/2}\text{Cf}_x$ approaches to ξ and the values of coefficient magnetic intensity $\text{Re}_x^{1/2}\text{Mg}_x$ approaches to ξ/Pm and Nusselt number $\text{Re}_x^{-1/2}\text{Nu}_x$ approaches to $[1+(4/3R_d)(1+\Delta\theta_0)^3]\text{Pr}\xi$. The comparison of the present results with the numerical results obtained by FDM shows excellent agreement in the down stream region.

5. Conclusion

The physical parameters such as mixed convection parameter λ, transpiration parameter ξ, magnetic field parameter S, magnetic Prandtl number Pm and radiation parameter R_d, Prandtl number Pr and surface temperature θ_w exerts significant influence on coefficients of skin friction $\mathrm{Re}_x^{1/2}\mathrm{Cf}_x$, heat transfer $\mathrm{Re}_x^{-1/2}\mathrm{Nu}_x$ and magnetic intensity $\mathrm{Re}_x^{1/2}\mathrm{Mg}_x$ at the surface.

(i) The coefficient of skin friction decreases, and the coefficient of rate of heat transfer and magnetic intensity at the surface increases with the increase of radiation parameter R_d.

(ii) The coefficients of skin friction, heat transfer increases and magnetic intensity at the surface decreases with the increase of mixed convection parameter λ by keeping radiation parameter R_d, surface temperature θ_w, magnetic Prandtl Pm, magnetic force parameter S fixed. The momentum and thermal boundary layer thicknesses decreases and velocity and temperature profiles increases with the increase of the mixed convection parameter λ. It is also noted that the increase in mixed convection parameter λ reduce the transverse component of magnetic field profile.

(iii) The increase in Prandtl number Pr reduce the coefficient of skin friction and enhance the coefficient of heat transfer and magnetic intensity at the surface.

(iv) The coefficient of skin friction, heat transfer increases and the coefficient of magnetic intensity decreases with the increase of magnetic Prandtl number Pm.

(v) The transpiration parameter ξ play a significant role in boundary layer, due to increase in transpiration parameter ξ the momentum and thermal boundary layer thicknesses decreases and the transverse component of magnetic field profile also reduced.

(vi) It is also concluded that an increase of the conduction radiation parameter R_d decrease the local velocity as well as temperature distribution and enhance the transverse component of magnetic field at the surface.

Nomenclature

U_0: Reference velocity, $\mathrm{m \cdot s^{-1}}$
U_∞: Free stream velocity, $\mathrm{m \cdot s^{-1}}$
H_0: Reference magnetic field velocity
H_∞: Free stream magnetic field
S: Magnetic field parameter
f: Transformed stream function
Pm: Magnetic Prandtl number
Re_x: Local Reynolds number
Gr_x: Local Grashof number
Cf_x: Skin friction
H_x: Magnetic field along the surface
H_y: Magnetic field normal to the surface

Nu_x: Local Nusselt number
Mg_x: Magnetic intensity at the surface
u: Dimensional axial velocity, $\mathrm{m} \cdot \mathrm{s}^{-1}$
v: Dimensional normal velocity, $\mathrm{m} \cdot \mathrm{s}^{-1}$
T_w: Wall temperature, K
T_∞: Ambient fluid temperature, K
V_0: Surface mass flux
R_d: Plank number (radiation-conduction parameter)
x: Axial distance, m
y: Normal distance, m
g: Acceleration due to gravity, $\mathrm{m} \cdot \mathrm{s}^{-2}$.

Greek Letters

ψ: Fluid Stream function, $\mathrm{m}^2 \cdot \mathrm{s}^{-1}$
ϕ: Transformed stream function for magnetic field
ξ: Transpiration parameter
α: Thermal diffusivity, $\mathrm{m}^2 \cdot \mathrm{s}^{-1}$
λ: Mixed convection parameter
μ: Dynamical viscosity, $\mathrm{Kg} \cdot \mathrm{m}^{-1} \cdot \mathrm{s}^{-1}$
η: Similarity transformation
ν: Kinematic viscosity, $\mathrm{m}^2 \cdot \mathrm{s}^{-1}$
θ: Dimensionless temperature function
θ_w: Surface temperature ratio to the ambient fluid
ρ: Density of the fluid, $\mathrm{Kg} \cdot \mathrm{m}^{-3}$
σ: Electrical conductivity, $S(siemens) \cdot \mathrm{m}^{-1}$
σ_s: Stefan-Boltzman constant
γ: Magnetic diffusion
β: Coefficient of cubical expansion
$\overline{\mu}$: Magnetic permibility.

Subscripts

w: Wall condition
∞: Ambient condition.

References

[1] H. P. Greenspan and G. F. Carrier, "The magnetohydrodynamic flow past a flat plate," *Journal of Fluid Mechanics*, vol. 6, pp. 77–96, 1959.

[2] T. V. Davies, "The magneto-hydrodynamic boundary layer in the two-dimensional steady flow past a semi-infinite flat plate. I. Uniform conditions at infinity," *Proceedings of the Royal Society of London A*, vol. 273, pp. 496–508, 1963.

[3] T. V. Davies, "The magneto-hydrodynamic boundary layer in the two-dimensional steady flow past a semi-infinite flat plate. III. The influence of an adverse magneto-dynamic pressure gradient," vol. 273, pp. 518–537, 1963.

[4] R. J. Gribben, “Magnetohydrodynamic stagnation-point flow,” *Quarterly Journal of Mechanics and Applied Mathematics*, vol. 18, no. 3, pp. 357–384, 1963.

[5] R. J. Gribben, “Magnetohydrodynamic boundary layers in presence of pressure gradient,” *Proceedings of the Royal Society of London A*, vol. 287, pp. 123–141, 1965.

[6] P. Ramamoorthy, “Heat transfer in hydromagnetics,” *The Quarterly Journal of Mechanics and Applied Mathematics*, vol. 18, pp. 31–40, 1965.

[7] C. W. Tan and C. C. T. Wang, “Heat transfer in aligned-field magnetohydrodynamic flow past a flat plate,” *International Journal of Heat and Mass Transfer*, vol. 11, no. 2, pp. 319–329, 1967.

[8] L. T. Hildyard, “Falkner-Skan problem in magnetohydrodynamics,” *Physics of Fluids*, vol. 15, no. 6, pp. 1023–1027, 1972.

[9] S. S. Chawla, “Magnetohydrodynamic oscillatory flow past a semi-infinite flat plate,” *International Journal of Non-Linear Mechanics*, vol. 6, no. 1, pp. 117–134, 1971.

[10] D. B. Ingham, “The magnetogasdynamic boundary layer for a thermally conducting plate,” *Quarterly Journal of Mechanics and Applied Mathematics*, vol. 20, no. 3, pp. 347–364, 1967.

[11] M. B. Glauert, “The boundary layer on a magnetized plate,” *Journal of Fluid Mechanics*, vol. 12, pp. 625–638, 1962.

[12] S. S. Chawla, “Fluctuating boundary layer on a magnetized plate,” *Proceedings of the Cambridge Philosophical Society*, vol. 63, p. 513, 1967.

[13] M. M. Ali, T. S. Chen, and B. F. Armaly, “Natural convection radiation interaction in boundary layer flow over horizontal surface,” *AIAA Journal*, vol. 22, no. 12, pp. 1797–1803, 1984.

[14] V. S. Arpaci, “Effect of thermal radiation on the laminar free convection from a heated vertical plate,” *International Journal of Heat and Mass Transfer*, vol. 15, pp. 1243–1252, 1972.

[15] E. H. Cheng and M. N. Özişik, “Radiation with free convection in an absorbing, emitting and scattering medium,” *International Journal of Heat and Mass Transfer*, vol. 15, no. 6, pp. 1243–1252, 1972.

[16] E. M. Sparrow and R. D. Cess, “Radiation heat transfer, Aumented edition, Hemisphere media,” *International Journal of Heat and Mass Transfer*, vol. 5, pp. 179–806, 1962.

[17] V. M. Soundalgekar, H. S. Takhar, and N. V. Vighnesam, “Combined free and forced convection flow past a semi-infinite vertical plate with variable surface temperature,” *Nuclear Engineering and Design*, vol. 110, no. 1, pp. 95–98, 1988.

[18] M. A. Hossain and H. S. Takhar, “Radiation effect on mixed convection along a vertical plate with uniform surface temperature,” *Heat and Mass Transfer*, vol. 31, no. 4, pp. 243–248, 1996.

[19] N. C. Roy and M. A. Hossain, “The effect of conduction-radiation on the oscillating natural convection boundary layer flow of viscous incompressible fluid along a vertical plate,” *Proceedings of the Institution of Mechanical Engineers C*, vol. 224, no. 9, pp. 1959–1972, 2010.

[20] E. M. Aboeldahab and M. S. El Gendy, “Radiation effect on MHD free-convective flow of a gas past a semi-infinite vertical plate with variable thermophysical properties for high-temperature differences,” *Canadian Journal of Physics*, vol. 80, no. 12, pp. 1609–1619, 2002.

[21] P. Mebine and E. M. Adigio, “Unsteady free convection flow with thermal radiation past a vertical porous plate with newtonian heating,” *Turkish Journal of Physics*, vol. 33, no. 2, pp. 109–119, 2009.

[22] G. Palani and I. A. Abbas, “Free convection MHD flow with thermal radiation from an impulsively-started vertical plate,” *Nonlinear Analysis: Modelling and Control*, vol. 14, no. 1, pp. 73–84, 2009.

[23] R. Eichhorn, “The effect of mass transfer on free convection,” *Journal of Heat Transfer*, vol. 82, pp. 260–263, 1960.

[24] E. M. Sparrow and R. D. Cess, “Free convection with blowing or suction,” *Journal of Heat Transfer*, vol. 83, pp. 387–396, 1961.

[25] J. H. Merkin, “The effects of blowing and suction on free convection boundary layers,” *International Journal of Heat and Mass Transfer*, vol. 18, no. 2, pp. 237–244, 1975.

[26] J. F. Clarke, “Transpiration and natural convection: the vertical plate problem,” *Journal of Fluid Mechanics*, vol. 57, no. 1, pp. 45–61, 1973.

[27] M. Vedhanayagam, R. A. Altenkrich, and R. Eichhorn, “A transformation of the boundary layer equations for free convection past a vertical flat plate with arbitrary blowing and wall temperature variations,” *International Journal of Heat and Mass Trasfer*, vol. 23, pp. 1286–1288, 1980.

[28] J. F. Clarke and N. Riley, “Natural convection induced in a gas by the presence of a hot porous horizontal surface,” *Quarterly Journal of Mechanics and Applied Mathematics*, vol. 28, no. 4, pp. 373–396, 1975.

[29] H. T. Lin and W. S. Yu, “Free convection on a horizontal plate with blowing and suction,” *Journal of Heat Transfer*, vol. 110, no. 3, pp. 793–796, 1988.